

## Molecular exchange and percolation in 2D-nanoparticle arrays

Sense Jan van der Molen<sup>#</sup>, Jianhui Liao, Laetitia Bernard<sup>&</sup>, Christian Schönenberger, Michel Calame<sup>\*</sup>

*Institut für Physik, Universität Basel, Klingelbergstrasse 82, CH-4056 Basel, Switzerland*

RECEIVED DATE (automatically inserted by publisher); \*michel.calame@unibas.ch

The role of kinetic aspects in molecular junction formation remains to date widely unexplored, despite its importance in molecular electronics.<sup>1</sup> Recently, we demonstrated the reversible insertion of conjugated dithiol-molecules in 2D-arrays of alkanethiol-covered gold nanoparticles.<sup>2</sup> The incoming dithiolated molecules partially replace the alkanethiols, leading to molecular bridge formation. At the end of this process, the resistance of the device has dropped by a few orders of magnitude. Since the arrays contain many metal-molecule-metal junctions, they offer a robust platform to determine average properties of molecular junctions. Here, we focus on the dynamics of the insertion process. We study the insertion kinetics by monitoring the conductance of 2D-networks as a function of the time they spent in a solution containing dithiolated molecules. From the data, we derive the combined kinetics of molecular place exchange and bridging between gold electrodes. The evolution of the relative number of bridges forming during exchange is deduced in the framework of a percolation theory. In this work, we focus specifically on the insertion process of dithiolated oligo(phenylene-ethynylene) (OPE) bridges at three distinct temperatures.<sup>2</sup>

Two-dimensional nanoparticle arrays were created by self-assembling octanethiol-covered gold nanoparticles at the air/water interface.<sup>2,3</sup> Using a stamping procedure and subsequent gold contact evaporation, we produced three substrates, each containing tens of individual network devices.<sup>2</sup> Immediately after preparation, we measured the conductance of ten devices on each substrate. We then started the exchange process. For this, we immersed a substrate in 1 mM of deprotected OPE in Ar-bubbled THF at a temperature  $T$ . After a well-defined time interval, we took it out, rinsed it in THF and quickly dried it in a  $N_2$  gas flow. Next, the conductance of the devices was measured in the ambient, followed by another exchange step. Repeating this procedure, we determined the conductance  $G$  of each device as a function of exchange time  $t$ . We performed the exchange process on the three substrates at different temperatures ( $0^\circ\text{C}$ ,  $25^\circ\text{C}$  and  $40^\circ\text{C}$ ), with  $t$  running from 5 minutes to a final time  $t_f \sim 1$  day.

In the inset of Fig. 1a, we show four typical curves of  $G$  versus  $t$  at  $T=25^\circ\text{C}$ . They all have a similar shape, i.e., an increase of  $G$  by more than two orders of magnitude is observed, after which the curves flatten off. The saturation values depend somewhat on the specific sample, as reported before.<sup>2</sup> This reflects the sensitivity of the conductance to the particular nanoparticle arrangement in each device. Nevertheless, the similarity of the curves suggests a universal behavior of all data sets. To obtain a balanced average curve for all samples at  $T=25^\circ\text{C}$ , we use the following procedure. First, we normalize each data set to the final conductance value, i.e., we define  $G_{\text{norm}}(t) \equiv G(t)/G(t_f)$ . Then, we calculate the average  $G_{\text{norm}}(t)$  curves for all devices. In this way, each data set has an equal weight. The same procedure is used for the devices measured at  $0^\circ\text{C}$  and  $40^\circ\text{C}$ . In Fig. 1a, we show the

averaged  $G_{\text{norm}}(t)$  curves for all temperatures. Clearly, the conductance increases faster with time as the temperature is raised. We also note that the average ratio of the final and initial conductance values,  $G(t=t_f)/G(t=0)$ , is similar for all  $T$ , i.e., 250, 400 and 500 for  $0^\circ\text{C}$ ,  $25^\circ\text{C}$  and  $40^\circ\text{C}$ , respectively. The somewhat lower value for  $T=0^\circ\text{C}$  however, indicates that full saturation might have not been reached in that case. It is for this reason that we took an extra data point at this temperature ( $t_f=1975$  minutes).

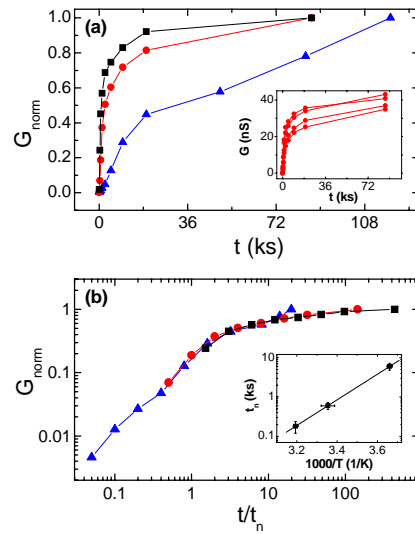


**Figure 1.** (a) Normalized conductance  $G_{\text{norm}}$  versus time  $t$  during exchange at three temperatures  $T$ :  $\blacktriangle$ :  $0^\circ\text{C}$ ,  $\bullet$ :  $25^\circ\text{C}$  and  $\blacksquare$ :  $40^\circ\text{C}$ . Inset: absolute conductance  $G$  vs  $t$  for four data sets at  $25^\circ\text{C}$ . (b)  $G_{\text{norm}}$  vs normalized time,  $t/t_n(T)$ . All data sets collapse onto one curve for  $t_n(0^\circ\text{C})=6000$  s,  $t_n(25^\circ\text{C})=600$  s and  $t_n(40^\circ\text{C})=180$  s, respectively. Inset: Arrhenius plot of  $t_n$ . From this we deduce an activation energy of  $(6 \pm 1) \times 10^4$  J/mol.

To understand these data, we need to consider the relation between conductance and molecular bridge formation further. At  $t=0$ , the conductance of a device,  $G_0$ , is determined by tunneling through octanethiols.<sup>2</sup> During the exchange process, octanethiols are progressively replaced by OPE-dithiols and more and more molecular junctions, with a relatively high local conductance, are formed. Once a continuous path of OPE-bridged junctions runs from source to drain,  $G$  rises dramatically. Such a 'percolation' path emerges when a fraction  $p=p_c$  of all nanoparticle pairs is bridged by OPE. Percolation phenomena have been the subject of intensive study in the past.<sup>4</sup> Specifically, for 2D-hexagonal networks, a bond percolation threshold at  $p_c=2 \cdot \sin(\pi/18) \approx 0.35$  has been found.<sup>4(e)</sup> The evolution of the conductance during exchange is determined by two processes: i) by the temperature-dependent kinetics of molecular exchange and bridging, i.e., the fraction  $p$  of OPE-bridged nanoparticle pairs increases continuously with time; ii) by percolation, i.e., each value of  $p$

defines a network conductance  $G$  via a percolation relation.<sup>4</sup> Formally, this yields:  $G_{\text{norm}}(t, T) = G_{\text{norm}}(p(t, T))$ . Hence, the temperature dependence in Figure 1a is directly related to the bridging kinetics. The strong similarity between the three curves suggests that the dominant mechanism of exchange and bridging is the same at all temperatures. To test this hypothesis, we use the following procedure. For each  $G_{\text{norm}}(t)$  curve, we normalize the  $t$ -scale by a temperature-dependent factor  $t_n(T)$ . We take  $t_n$ , rather arbitrarily, such that  $G_{\text{norm}}=0.15$  when  $t/t_n=1$ . In Figure 1b, we show  $G_{\text{norm}}(t/t_n)$  for all data sets. Indeed, the data collapse onto a ‘universal’ curve, confirming our hypothesis. The inset of Figure 1b displays an Arrhenius plot of  $t_n(T)$ . It shows that the kinetics is dominated by an activated process with a barrier of  $(6\pm 1)\times 10^4$  J/mol or  $0.6\pm 0.1$  eV per molecule. A comparison to recent investigations of the thermally activated breakdown of molecular junctions is worthwhile.<sup>5(a),5(b)</sup> A most probable binding energy of  $\approx 0.7$ eV was found there for Au-alkanethiols junctions measured via conducting atomic force microscopy. We expect that the process resulting in the bridging of adjacent nanoparticles is complex and probably multi-step. The above discussion yet indicates that the dominant, rate-limiting barrier might be the metal-molecule bond. Note that the energy value obtained is typical for the strength of a Au-Au bond.<sup>5(c)</sup> This means that a detached molecule probably pulled away a Au atom from the electrode.<sup>5(a)</sup> Upon multiple exchanges, an etching of the nanoparticles might therefore take place.<sup>5(d)</sup> It is nonetheless remarkable that the binding energy value was determined here from conductance measurements only, demonstrating the strength of this simple method.

Using the ‘universal’ curve in Figure 1b, we extend our method further to deduce the kinetics of exchange and bridging. For this, we need to obtain  $p(t/t_n)$  from  $G(t/t_n)$ , using percolation theory. The general effective medium equation has proven to give a successful relation between  $G$  and  $p$ .<sup>4(b),4(c)</sup> For a 2D-system, it reads:

$$\frac{(1-p)(G_0^{3/4} - G^{3/4})}{G_0^{3/4} + A_c \cdot G^{3/4}} + \frac{p(G_1^{3/4} - G^{3/4})}{G_1^{3/4} + A_c \cdot G^{3/4}} = 0 \quad (1)$$

Here,  $G_0 = G(p=0)$  (conductance before exchange),  $G_1 = G(p=1)$  (conductance at full exchange) and  $A_c = (1-p_c)/p_c = 1.88$ . From equation (1) we derive the relation  $p(G)$  explicitly and apply it to the  $G_{\text{norm}}(t/t_n)$ -curve in Figure 1b. The resulting kinetics relation of  $p$  versus  $t/t_n$  is shown in Figure 2a. We see by interpolation that at  $t/t_n=0.3$ , we have  $p=p_c=0.35$ . The percolation threshold is thus reached relatively fast.

The relation  $p(t/t_n)$  allows us to test various kinetic models for molecular exchange on nanoparticles.<sup>6</sup> We first compare our data with 1<sup>st</sup>-order Langmuir kinetics, i.e.  $p(t) = 1 - \exp(-at^q)$ , with  $q=1$  or  $q=0.5$  (diffusion-limited case). These attempts are not successful (See Suppl. Info). For 2<sup>nd</sup>-order Langmuir kinetics, one expects:  $p(t) = at^q/(1+at^q)$ , with  $q=1$  or  $q=0.5$ . This can be rewritten as  $p/(1-p) = at^q$ . In Figure 2b, we show  $p/(1-p)$  versus  $t/t_n$  in a log-log plot. As expected for 2<sup>nd</sup>-order Langmuir kinetics, a linear relation is found over more than three decades in  $t/t_n$ . We derive an exponent of  $q=0.6$ . This is close to 0.5, pointing towards an exchange and bridging process governed by diffusion-limited 2<sup>nd</sup>-order Langmuir kinetics. Interestingly, similar kinetics was found for the place exchange of alkanethiols on nanoparticles in solution.<sup>6(d)</sup> This suggests that the exchange step is rate-limiting in 2D-networks, while the bridging step is not. Our preceding argument based on the activation energy is therefore reinforced.

In the procedure above, we assume full saturation of single molecular bonds at  $t=t_r$ . This assumption is probably too

optimistic. One reason for this is the existence of defects and grain boundaries in the hexagonal nanoparticle lattice.<sup>2</sup> If neighboring nanoparticles are too far apart, molecular bridging becomes impossible. Furthermore, optical spectroscopy studies on our samples indicate that around 30% of the alkanethiols are replaced after exchange.<sup>2(b)</sup> Most likely, only the vertex and edge sites allow for place exchange.<sup>6(a),6(b)</sup> We however show that the assumption of full exchange can be loosened. If we assume a final value  $p(t_r) = 0.5$ , the conclusions above still hold (see Suppl. Info). We also note that some nanoparticle pairs may be bridged by multiple molecules. This is ignored here, since the relative change of conductance due to multiple bridging is small compared to the overall increase in conductance. However, it may play a role at large  $t/t_n$ , leading to a slower saturation of the conductance.

In summary, the kinetics of molecular exchange and bridging in 2D-nanoparticle networks has been inferred from conductance measurements. Specifically, we find that OPE-dithiol insertion in octane-monothiol networks follows an activated behavior with a barrier of  $(6 \pm 1)\times 10^4$  J/mol. In the framework of a percolation model, diffusion-limited 2<sup>nd</sup>-order Langmuir kinetics fits best to our data. This approach has a general applicability. It allows for systematic studies of place exchange and bridging in molecular devices at various temperatures and concentrations.

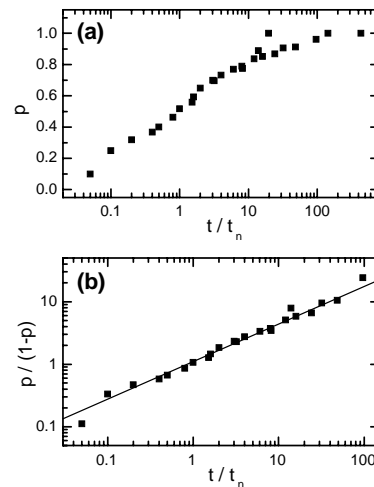


**Figure 2.** (a) The fraction of OPE-bridged nanoparticle-nanoparticle junctions,  $p$ , vs normalized time  $t/t_n$ . We derive this plot from Figure 1b and eq. (1). (b)  $p/(1-p)$  vs  $t/t_n$  on a log-log scale. For 2<sup>nd</sup>-order Langmuir kinetics, a straight line is expected, with a slope of 1 or 0.5 (diffusion limited). A linear fit to the data gives a slope of 0.6, close to the diffusion limited case.

<sup>#</sup> Present address: Kamerlingh Onnes laboratory, Leiden University, Niels Bohrweg 2, 2333 CA Leiden, the Netherlands.

<sup>&</sup> Present address: Department of Electrical Engineering, Yale University, CT-06520-8284 New Haven, USA.

**ACKNOWLEDGMENT** This work is supported by the Swiss National Center of Competence in Research ‘‘Nanoscale Science’’, the Swiss National Science Foundation, and the European Science Foundation via the Eurocore program on Self-Organized Nanostructures (SONS). SJvdM acknowledges the Netherlands Organisation for Scientific Research, NWO (‘Talent stipendium’).

**SUPPORTING INFORMATION:** Additional analysis.

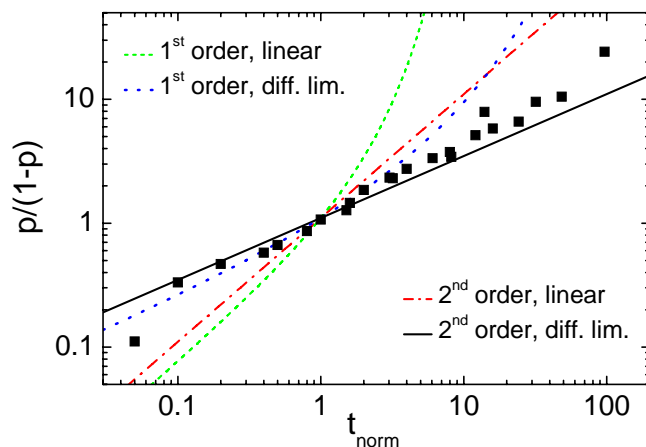
1. (a) Reichert, J.; Ochs, R.; Beckmann, D.; Weber, H.B.; Mayor, M.; Löhneysen, H.v. *Phys. Rev. Lett.* **2002**, *88*, 176804. (b) Nitzan A., Ratner, M. *Science* **2003**, *300*, 1384. (c) Xu, B., and Tao, N.J. *Science* **2003**, *301*, 1221-1223. (d) Gonzalez, M.T.; Wu, S.; Huber, R.; van der Molen, S.J.; Schönenberger, C.; Calame, M. *Nano Lett.* **2006**, *6*, 2238-2242. (e) Lindsay, S., Ratner, M. *Adv. Mat.* **2007**, *19*, 23-31.
2. (a) Liao, J.; Bernard, L.; Langer, M.; Schönenberger, C.; Calame, M. *Adv. Mater.* **2006**, *18*, 2444-2447; (b) Bernard, L.; Kamdzhilov, Y.; Calame, M.; van der Molen, S.J., Liao, J. and Schönenberger, C., *submitted*.
3. (a) Slot, J.W. and Geuze, H.J., *Eur. J. Cell Biol.* **1985**, *38*, 87. (b) Santhanam, V. and Andres, R.P., *Nano Lett.* **2004**, *4*, 41
4. (a) Kirkpatrick, S., *Rev. Mod. Phys.* **1973**, *45*, 574-588. (b) McLachlan, D.S. *J. Am. Ceram. Soc.* **1990**, *73*, 2187-2203. (c) Wu, J.; McLachlan, D.S. *Phys. Rev. B* **1997**, *56*, 1236-1248. (d) Lebovka, N.I.; Tarafdar, S.; Vygornitskii, N.V. *Phys. Rev. E* **2006**, *73*, 031402. (e) Wierman, J.C., *Adv. Appl. Probab.* **1981**, *13*, 298.
5. (a) Huang, Z., Chen, F., Bennett, P.A. and Tao, N. *Nano Lett.* **2006**, *6*, 1240-1244. (b) Huang, Z., Chen, F., Bennett, P.A., Tao, N., *submitted*. (c) Todorov, T.N., Hoekstra, J., and Sutton, A.P., *Phys. Rev. Lett.* **2001**, *86*, 3606-3609. (d) Schönenberger, C., Sondag-Huethorst, J.A.M., Jorritsma, J. and Fokkink, L.G.J., *Langmuir* **1994**, *10*, 611-614.
6. (a) Hostetler, M. J., Templeton, A. C. and Murray, R.W. *Langmuir* **1999**, *15*, 3782. (b) Song, Y. and Murray, R.W. *J. Am. Chem. Soc.* **2002**, *124*, 7096-7102. (c) Hong, R.; Fernandez, J.M.; Nakade, H.; Arvizo, R.; Emrick, T.; Rotello, V.M. *Chem. Commun.* **2006**, 2347-2349. (d) Kassam, A.; Bremner, G.; Clark, B.; Ulibarri, G.; Lennox, R.B. *J. Am. Chem. Soc.* **2006**, *128*, 3476-3477.

# Supplementary Information

## Molecular exchange and percolation in 2D-nanoparticle arrays

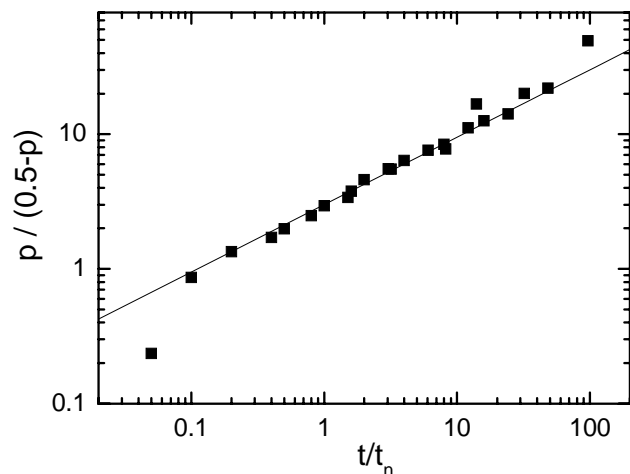
Sense Jan van der Molen, Jianhui Liao, Laetitia Bernard, Christian Schönenberger, Michel Calame  
Institut für Physik, Universität Basel, Klingelbergstrasse 82, CH-4056 Basel, Switzerland

Figure S1 compares the four different Langmuir kinetics models described in the text. The data are those shown in Figure 2. A diffusion-limited, 2<sup>nd</sup> order Langmuir model gives the best correspondence to the data (black curve). The curve is shown for  $q=0.5$  as the model predicts. A fit to the data (Figure 2) gives  $q=0.6$ .

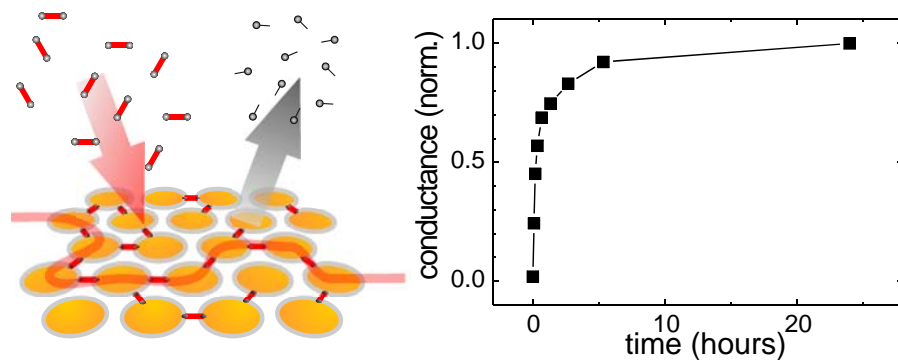


**Fig. S1** Log-log plot of  $p/(1-p)$  versus time, compared to four Langmuir models. Green curve: 1<sup>st</sup> order, linear; blue curve: 1<sup>st</sup> order, diffusion limited; red curve: 2<sup>nd</sup> order, linear; black curve: 2<sup>nd</sup> order, diffusion limited

To test whether we can loosen the assumption of full saturation at  $t=t_f$ , we force  $p(t_f)=0.5$  and obtain a new set of  $p(t)$  values from Figure 1b. We show in Figure S2 that diffusion-limited, 2<sup>nd</sup> order Langmuir kinetics gives again a good correspondence to our data. A fit to this data set according to  $p(t)=at^q/(1+at^q)$  gives  $q=0.5$ , the value expected. We find  $q=0.6$  when assuming full saturation (Figure 2).



**Fig. S2** Same data as in Figure 1, assuming that only half of the bonds are saturated after the final exchange step, i.e.:  $p=0.5$  at  $t=t_f$ . AS in Figure 2, we plot  $p/(0.5-p)$  versus time on log-log scales. A fit using 2<sup>nd</sup> order Langmuir kinetics still describes our data adequately (line).



ABSTRACT FOR WEB PUBLICATION

We study the kinetics of molecular exchange and bridging in 2D nanoparticles networks, based on conductance measurements and percolation theory. Specifically, we follow, at different temperatures, the insertion of di-thiolated oligo(phenyle ethynylene) compounds in stamped octanethiol-capped Au nanoparticle networks. This process is found to take place according to a diffusion-limited, 2<sup>nd</sup> order Langmuir kinetics and exhibits an activated behavior with a barrier of  $(6 \pm 1) \times 10^4$  J/m.